Journal of Applied Polymer Science

Modification of SPPESK proton exchange membranes through layer-by-layer self-assembly

Yuanyuan Sun, Xuemei Wu, Dongxing Zhen, Shikai Zhang, Mengmeng Hu, Gaohong He
State Key Laboratory of Fine Chemicals, Research and Development Center of Membrane Science and Technology, Department of Chemical Engineering, Dalian University of Technology, Dalian, LN 116024, China
Correspondence to: G. He (E-mail: hgaohong@dlut.edu.cn)

ABSTRACT: Sulfonated poly(phthalazinone ether sulfone ketone) (SPPESK) composite membranes are fabricated through electrostatic layer-by-layer (LbL) self-assembly method with chitosan (CS) and phosphotungstic acid (PWA) to enhance the proton conductivity and stability. The results demonstrate that LbL self-assembly has different effects on the SPPESK membrane substrates with different sulfonation degrees (DSs). It elevates proton conductivity of the SPPESK membrane of lower DS and enhances swelling stability of the SPPESK membrane of higher DS. For instance, at 80°C, proton conductivity of the SPPESK0.74/$(CS/PWA)_1$ membrane (lower DS) increases by 16%–96.49 mS cm^{-1}, and swelling ratio of the SPPESK1.01/$(CS/PWA)_3$ membrane (higher DS) decreases from 58 to 29%. Attribute to the electrostatic interaction and ion cross-linking networks, permeability of the SPPESK0.74/$(CS/PWA)_3$ membrane and the SPPESK1.01/$(CS/PWA)_5$ membrane are reduced by 45 and 30%, respectively. The results indicate that the LbL self-assembly has broadened the available DS range for fuel cell applications. © 2015 Wiley Periodicals, Inc. J. Appl. Polym. Sci. **2016**, *133*, 42867.

KEYWORDS: batteries and fuel cells; membranes; polyelectrolytes; self-assembly

Received 6 April 2015; accepted 24 August 2015
DOI: 10.1002/app.42867

INTRODUCTION

Proton exchange membrane fuel cell (PEMFC) has been extensively studied as an electrochemical energy conversion device due to high power density, compactness and environmental friendliness.[1,2] As the core component of PEMFC, proton exchange membrane (PEM) acts as not only a separator between the fuel and oxidant, but also the proton-conductive medium from anode to cathode.[3–5] Nafion, a perfluorinated membrane, has been considered to be the state-of-the-art PEM in PEMFCs for superior proton conductivity. However, high methanol permeability and excessive cost limit its further development,[6,7] thus stimulating the efforts to investigate inexpensive and environmentally friendly nonfluorinated polymers.[8]

Sulfonated poly(phthalazinone ether sulfone ketone) (SPPESK) has great prospects for PEM applications due to its excellent chemical durability and mechanical properties.[9] However, in comparison with perfluorinated membranes, SPPESK PEM exhibits weaker acidity, narrower ion-channel and more "dead ends."[10] Consequently, competitive conductivity must be attained by increasing the sulfonation degree (DS), that is, the ion exchange capacity (IEC).[11] Unfortunately, the dimensional stability and methanol resistance will be deteriorated with higher DS.[12] Therefore, a balance must be achieved between the conductivity and stability. To solve this problem, significant efforts such as covalent crosslinking,[13] semi-interpenetrating,[14] and doping organically modified montmorillonite[15] had been performed in our previous works. In addition, Nagarale *et al.*[16] polymerized a thin layer of polyaniline (PANI) on the surface of the SPEEK membrane to enhance the stability and methanol resistance. However, all the improvements are still at the cost of declining in proton conductivity.

Electrostatic layer-by-layer (LbL) self-assembly shows great potential in the preparation and modification of PEMs in recent years because of the advantages of simple operation, environmental friendliness and high versatility.[17–19] Through sequential electrostatic adsorption between the positively and negatively charged polyelectrolytes, highly ordered structure is constructed spontaneously.[20,21] It has been proved superior in methanol resistance in consequence of the multilayer on the membrane substrate.[22,23] Proton conductivity can also be enhanced by choosing a proper combination of polycation and polyanion.[24] For instance, a multilayer film of PANI and phosphotungstic acid (PWA) elevated the proton conductivity of the substrate membrane from 0.074 S cm^{-1} (25°C) to 0.093 S cm^{-1}.[25]

Despite the great application potential of the LbL self-assembly in PEMs,[26,27] no information is available on SPPESK LbL self-assembly membrane in literature so far. Moreover, most relative studies put emphasis merely on the influence of polyelectrolyte

multilayer,[28,29] pH,[30] and ionic strength.[31] Little is known about the effects of DS of substrate membrane on the performance of PEMs. In this study, a multilayer is prepared on surface of the SPPESK membrane using electrostatic LbL self-assembly to improve the conductivity and stability. PWA, a super ionic conductor in fully hydrated states, is selected as the polyanion.[32,33] And CS acts as the polycation due to its affinity to water.[34,35] The effects of the multilayer film combined with DS on the performance are investigated in details.

EXPERIMENTAL

Materials

PPESK with a sulfone/ketone ratio of 1:1 (S/K = 1/1) was provided by Dalian Baolimo Chemicals and dried overnight at 120°C before use. Chitosan (CS, M_W = 500,000 and 90% degree of deacetylation), PWA (AR), sulfuric acid (96–98%, AR), fuming sulfuric acid (20–24% SO_3, AR), methanol (GR), n-butanol (GR), and other reagents were obtained commercially and used without further purification.

Preparation of SPPESK Membrane

SPPESK was synthesized by the direct sulfonation method using the mixture of sulfuric acid and fuming sulfuric acid as the sulfonating agent, and separated by precipitating in ice-cold deionized (DI) water. Details were reported in our previous work.[15] DS of SPPESK was determined by ion exchange titration. In this study, SPPESK with DS of 0.74 and 1.01 were used and named as SPPESK0.74 and SPPESK1.01, respectively.

The SPPESK membranes were prepared by solution casting from 10 wt % SPPESK in N-methyl-2-pyrrolidone (NMP). The SPPESK solution was purified by centrifugation for 15 min, and then casted onto a glass plate and dried at 60°C for 3 days. The dried membranes (about 50 μm) were soaked in 2 mol L^{-1} HCl solution for 48 h and washed with DI water to remove excess acid before usage.

LbL Self-Assembly on SPPESK Membrane Substrate

CS solution of 2 g L^{-1} (w/v) was prepared by dissolving CS in 2% (v/v) acetic acid solution and PWA was dissolved in DI water to form 1 mmol L^{-1} solution (pH 2.5). The LbL deposition process was carried out as follows. The prepared SPPESK membrane was dipped into CS solution at room temperature for 10 min and rinsed with DI water three times to remove weakly bonded electrolyte molecules, followed by removal of the residual water with absorbent tissue. Subsequently, the membrane was deposited with a PWA layer following the same steps adopted for CS deposition. The alternate self-assembly of CS and PWA was repeated to increase the number of CS/PWA bilayer on SPPESK membrane. The corresponding modified SPPESK membrane was denoted as SPPESK/(CS/PWA)*n* composite membrane, where *n* was the number of CS/PWA bilayer. In our work, SPPESK0.74 with 3 CS/PWA bilayers and SPPESK1.01 with 5 CS/PWA bilayers composite membranes were prepared to make sure both the membranes possess low enough swelling ratio and high enough conductivity at the same time.

LbL Self-Assembly Characterization

The Fourier transform infrared spectroscopy (FTIR) spectra was recorded on an EQUINOX55 FTIR instrument at a wave number range of 500–4000 cm^{-1}.

The morphology of the membranes was examined using a QUANTA450 scanning electron microscope (SEM). Prior to measurement, the samples were fractured in liquid nitrogen and sputter-coated with a thin layer of gold on the fractured section.

The IEC of the membranes was obtained by titration technique. Membrane samples were soaked into 3 mol L^{-1} NaCl solution for 24 h to ensure the fully exchange of Na^+ ions for H^+ ions. Then the solutions were titrated by 0.01 mol L^{-1} NaOH solution with phenolphthalein as the indicator. IEC was calculated as the following equation:

$$\mathrm{IEC} = \frac{V_{\mathrm{NaOH}} \times C_{\mathrm{NaOH}}}{M_{\mathrm{dry}}} \quad (1)$$

where *V*NaOH and *C*NaOH are the volume and concentration of NaOH solution, respectively, and M_{dry} is the dry weight of membrane samples.

Membrane Properties Characterization

Water uptake measurement was done by gravimetric technique. Membrane samples were immersed into DI water at a certain temperature for 12 h and measured the weight (m_{wet}) and dimension. After dried at 80°C for 24 h, the weight (m_{dry}) and dimension were redetermined. The water uptake and swelling ratio were calculated by the two following equations, respectively.

$$\text{Water uptake}(\%) = \frac{m_{\mathrm{wet}} - m_{\mathrm{dry}}}{m_{\mathrm{dry}}} \times 100\% \quad (2)$$

$$\text{Swelling ratio}(\%) = \frac{l_{\mathrm{wet}} - l_{\mathrm{dry}}}{l_{\mathrm{dry}}} \times 100\% \quad (3)$$

where $l\mathrm{wet} = (l\mathrm{wet1} \cdot l\mathrm{wet2})^{1/2}$, $l\mathrm{dry} = (l\mathrm{dry1} \cdot l\mathrm{dry2})^{1/2}$, and l_{wet1}, l_{wet2}, l_{dry1} and l_{dry2} are lengths and widths of wet membranes and dry membranes, respectively.

Proton conductivity was measured by the four-electrode AC impedance method using the Ivium A08001 impedance analyzer over a frequency range of 1–10^5 Hz. Conductivity (σ) was obtained using the following equation:

$$\sigma = \frac{L}{RdD} \quad (4)$$

where *L* is the distance between the two potential electrodes, *d* and *D* are the thickness and width of the membrane sample, respectively, and *R* is the resistance of membrane.

The methanol permeability was determined by a static method[15] using a home-made glass diffusion cell, where the membrane was sandwiched between two reservoirs. The left reservoir was filled with mixture of 1 mol L^{-1} methanol and 0.02 mol L^{-1} 1-butanol and the right reservoir had the same volume of 0.02 mol L^{-1} 1-butanol. With stirring on both sides, methanol in the left reservoir would diffuse into right gradually and the instant concentration of methanol in the right reservoir was obtained using gas chromatographic. According to the steady state principle, the relationship between the concentration of methanol in right reservoir and permeation time was given by:

$$\frac{dC_R}{dt} = \frac{AP}{LV}(C_L - C_R) \quad (5)$$

where V is the volume of solution in the reservoir, A and L are the area and thickness of the membrane, respectively, P is the methanol permeability, C_L is the pristine concentration of methanol in left reservoir, and C_R is the instant concentration of methanol in right reservoir. For the reasons of tiny permeation and no methanol existing in right reservoir at beginning, the equation $C_L - C_R \approx C_L$ is admissive. Herein, for eq. (5), the right section can be seen as constant (K), which is the slope of the concentration via time straight line. Therefore, an equation for methanol permeability as follows was obtained:

$$P = \frac{KLV}{AC_L} \quad (6)$$

The thermal stability of the membranes was analyzed using thermogravimetric analysis (TGA) following the process of 25°C-180°C-25°C-900°C at a rate of 10°C min^{-1} under a nitrogen atmosphere. Derivative thermogravimetry (DTG) curve was the first order derivative of TGA curve versus temperature.

RESULTS AND DISCUSSION

LbL Self-Assembly Characterization

Hammond[36] believed that the adsorbed polyelectrolyte multilayer thin layers were highly interpenetrated, and hence LbL self-assembly could be seen as a means of creating nanoscale blends. When the CS solution is added into PWA solution, white floc is formed, which is insoluble in either water or conventional solvents such as NMP. It is indicated that the electrostatic interaction between CS and PWA is strong enough to ensure the formation and stability of CS-PWA complex. The FTIR spectra of PWA, CS, and CS-PWA complex are presented in Figure 1, from which the characteristic peaks of both PWA and CS in CS-PWA complex are confirmed. For example, the bands at 1080, 982, 893, and 804 cm^{-1} are ascribed to v_{as} (P-O), v_{as} (W-O_d), v_{as} (W-O_b-W), and v_{as} (W-O_c-W) of PWA, respectively. Meanwhile, the wide bands at 3423 cm^{-1} derive from the overlapping of v_{as} (O—H) and v_{as} (N—H) of CS, and the peak at 1590 cm^{-1} is assigned to v_{as} (N—H). These adsorption peaks are not aggregated simply but exhibit blue or red shifts with changed widths, suggesting the existence of the strong electrostatic interaction between CS and PWA, and this is the basis of assembly. The results prove the preservation of geometry of PWA in the complex and thus ensure the function of conducting protons. It can be noticed that a new peak at 1521 cm^{-1} in the CS-PWA spectrum appears. This adsorption peak suggests the presence of amide group.[37] It should be formed from the reaction between CS and acetic acid during the preparation process of CS solution, which barely has effect on electrostatic interaction between CS and PWA.

Morphologies of the SPPESK/$(CS/PWA)_n$ composite membranes are investigated in detail. Figures 2 and 3 give the schematics and SEM images of the SPPESK1.01/$(CS/PWA)_5$ membrane, respectively. It is noticed in Figure 2 that a thin multilayer is constructed and coated on the surface of the SPPESK membrane substrate due to the electrostatic interaction. Figure 3(a) shows that there is a thin film (about 1.3 μm) deposited on surface of the SPPESK1.01 membrane substrate, demonstrating the success of the multilayer assembly. Figure 3(b) presents the clear structure of 1/2 bilayer, the thickness of which is about 130 nm. The surface morphology is smooth with no obvious phase separation [Figure 3(c)], confirming that PWA is entrapped or surrounded uniformly by CS chains because of the electrostatic interaction.

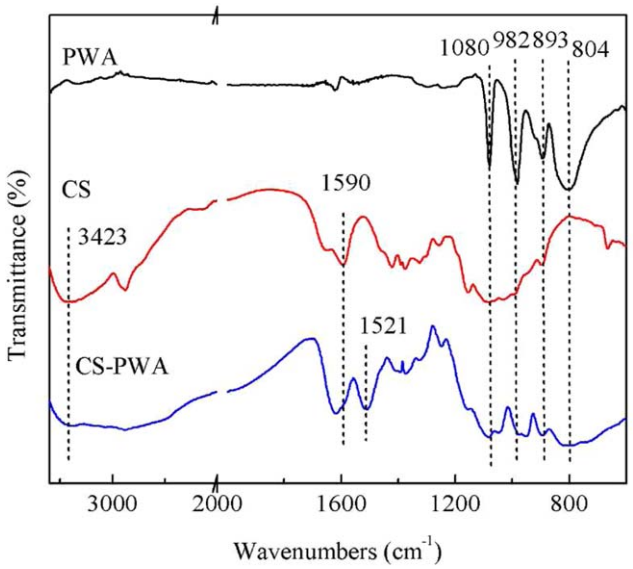

Figure 1. FTIR spectra of PWA, CS, and CS-PWA complex. [Color figure can be viewed in the online issue, which is available at wileyonlinelibrary.com.]

The IEC values of the SPPESK and SPPESK/$(CS/PWA)_n$ membranes are shown in Figure 4. It is noted that the IEC of the membranes decrease after LbL modification. The reason can be that some -SO_3H groups in SPPESK combined with CS could not exchange ions anymore and the low eigen IEC (0.03 mmol g^{-1}) of CS-PWA complex could not improve the overall IEC of the membrane. This verifies the success assembly of the multilayer on the membrane substrate in another aspect.

Membrane Properties

Water Uptake and Swelling Ratio. Water uptake is closely related to the proton conductivity and mechanical stability of membranes. High water uptake stimulates the transport of proton and thus elevates the efficiency of fuel cell, but excessive water may cause severe swelling and shorten the lifetime. Therefore, the optimal water uptake is essential to balance the conductivity and dimensional stability.[15,38] Water uptake and swelling ratio of the SPPESK and SPPESK/$(CS/PWA)_n$ membranes are shown in Figure 5(a,b), respectively. As shown, at 30°C, water uptake of the composite membranes with two different DSs increases firstly and then decreases with increasing bilayer numbers. For both DSs, the SPPESK/$(CS/PWA)_1$ membranes have the highest water uptake compared with other composite membranes. Despite that the combination of some —SO_3H groups with CS affects the uptake of water, CS and PWA are both strongly adsorbent and lead to the rising up of water uptake of the SPPESK/$(CS/PWA)_1$ membranes. With the increase of the bilayer number, the ion cross-linking networks

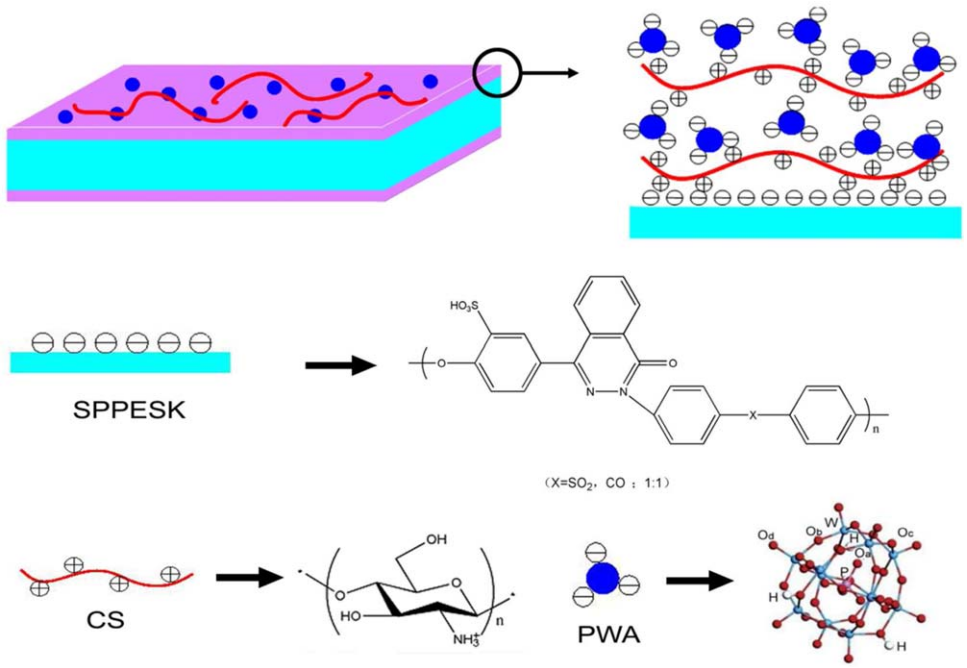

Figure 2. Schematics of the SPPESK/$(CS/PWA)_n$ composite membrane. [Color figure can be viewed in the online issue, which is available at wileyonlinelibrary.com.]

within the multilayer become denser, which reduces the uptake of water. The swelling ratio of the membranes behaves just as the water uptake. However, at 80°C, the LbL self-assembly shows significantly different modification effects on the substrate membranes with two different DSs. The SPPESK1.01/$(CS/PWA)_n$ membranes exhibit much lower water uptake and swelling ratio than the pristine membrane. For instance, the pristine SPPESK1.01 membrane has a water uptake of 148% and a swelling ratio of 58%, whereas those values of the SPPESK1.01/$(CS/PWA)_{2\text{-}5}$ membranes fall below 85 and 31%, respectively. The electrostatic interaction and the dense ion cross-linking networks within the multilayer dramatically inhibit the widening of pathways for water transport, restricting the uptake of water and the swelling behavior. In contrast, this restriction has little effects on the SPPESK0.74 membrane, which has relatively low swelling ratio and narrow pathways. Thus, the hydroscopic property of the multilayer is predominant, increasing the water uptake and swelling ratio of the pristine SPPESK0.74 membrane, just as at 30°C.

Proton Conductivity. Proton conduction is a key consideration when evaluating potential of membranes for fuel cell applications.[23,39] Figure 6 displays proton conductivity of the SPPESK and SPPESK/$(CS/PWA)_n$ membranes. It is shown that conductivity of the LbL self-assembly composite membranes increases firstly and then decreases with the increasing bilayer numbers. For both DSs, the SPPESK/$(CS/PWA)_1$ membranes exhibit the highest conductivity. However, the combination of $-SO_3H$ groups with CS is detrimental to proton conduction. However, the increasing water uptake of the composite membranes shown in Figure 5 and the strong proton donation nature of PWA are favorable to proton conduction. The overall effect is the improvement of conductivity. With increasing bilayer numbers, denser ion cross-linking networks restrict the uptake of water and the conductivity decreases ultimately. In addition, because of the different swelling behaviors shown in Figure 7, when constructing 3 bilayers, the SPPESK0.74/$(CS/PWA)_3$ membrane still shows higher conductivity at 80°C than the pristine SPPESK0.74 membrane, whereas conductivity of the SPPESK1.01/$(CS/PWA)_3$

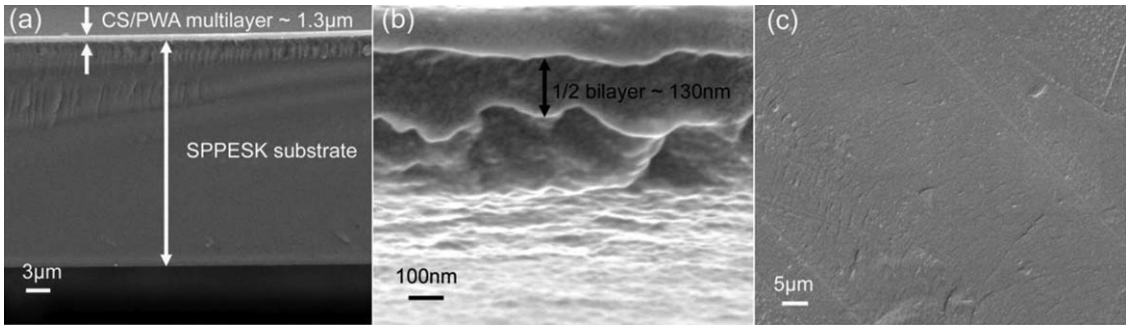

Figure 3. SEM images of the structure of the SPPESK1.01/$(CS/PWA)_5$ membrane: (a) the cross section of the SPPESK1.01/$(CS/PWA)_5$ membrane; (b) the cross section of 1/2 bilayer; (c) the surface morphology of the SPPESK1.01/$(CS/PWA)_5$ membrane.

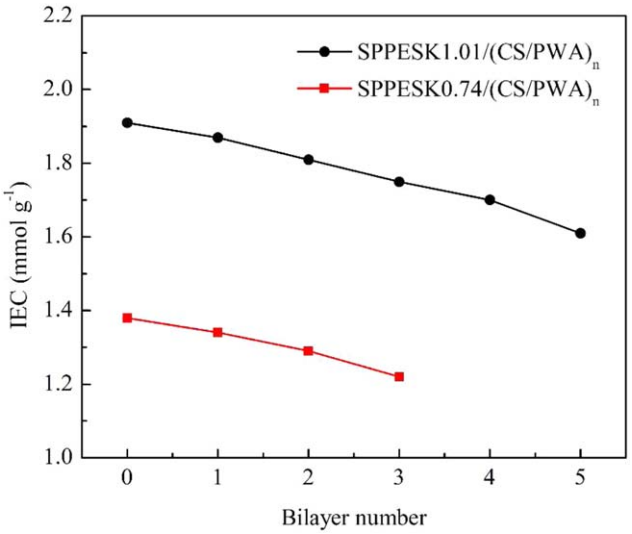

Figure 4. IEC values of the SPPESK and the SPPESK/(CS/PWA)$_n$ membranes. [Color figure can be viewed in the online issue, which is available at wileyonlinelibrary.com.]

membrane is slightly lower compared with the pristine SPPESK1.01 membrane.

A balance must be achieved between the conductivity and the mechanical stability. Taking both points into account, the LbL self-assembly has different modification effects on the SPPESK membrane substrate of different DSs. For lower DS of 0.74, when constructing 1 bilayer, the composite membrane exhibits the best performance. The conductivity reaches 96.49 mS cm^{-1} (80°C), 16% higher than that of the SPPESK0.74 membrane (83.34 mS cm^{-1}), and the swelling ratio is still below 20% despite slight increase. For higher DS of 1.01, when constructing 3 bilayers, the composite membrane is proved to be excellent. In contrast to the excessive swollen pristine SPPESK1.01 membrane (swelling ratio of 58% at 80°C), the SPPESK1.01/(CS/PWA)$_3$ membrane shows a swelling ratio of 29% with comparative proton conductivity. In a word, the LbL self-assembly elevates the conductivity of the membrane of lower DS and enhances the swelling stability of the membrane of higher DS. It can be concluded that the LbL self-assembly technique has broadened the available DS range for fuel cell applications.

Methanol Permeability

Methanol crossover not only results in the reduction of cell efficiency, but also poisons cathode catalysts.[40] Thus, low methanol permeability is expected. Methanol permeability of the SPPESK and the SPPESK/(CS/PWA)$_n$ membranes at 25°C are depicted in Figure 8. Apparently, the membranes with higher DS of 1.01 display faster methanol permeation. It is known that methanol is carried by H_3O^+ ion just as proton.[41] With higher DS, continuity of hydrophilic domains of SPPESK is improved by more water molecules and wider ion-channels, accelerating the diffusion of methanol.[42] Moreover, it is shown that methanol permeability of the composite membranes is lowered after LbL self-assembly modification and decreases as the number of bilayer increases. For instance, the SPPESK0.74/(CS/PWA)$_3$ membrane decreases by 45% to 1.4 × 10^{-7} cm^2 s^{-1} and the SPPESK1.01/(CS/PWA)$_5$ membrane decreases by 30% to 6.54 × 10^{-7} cm^2 s^{-1}. The results indicate that the electrostatic interaction between the multilayer and substrate and formation of ion cross-linking networks within the multilayer restrain the transport of methanol efficiently.

For the applications of PEMFCs, PEMs should have high proton conductivity and relatively low methanol permeability simultaneously. The selectivity, defined as the ratio of conductivity and permeability, is often used to evaluate the overall balance between them. Selectivity of the pristine and composite membranes is shown in Figure 9 and is compared with that of Nafion212 at the same time. It can be seen that the LbL self-assembly elevates the membrane selectivity, especially for lower DS. Furthermore, all membranes present a higher selectivity than Nafion212. For example, the SPPESK0.74/(CS/PWA)$_3$ membrane has the selectivity of 2.78 × 10^{-6} mS s cm^{-3}, 20 times higher than that of Nafion212, indicating that the LbL

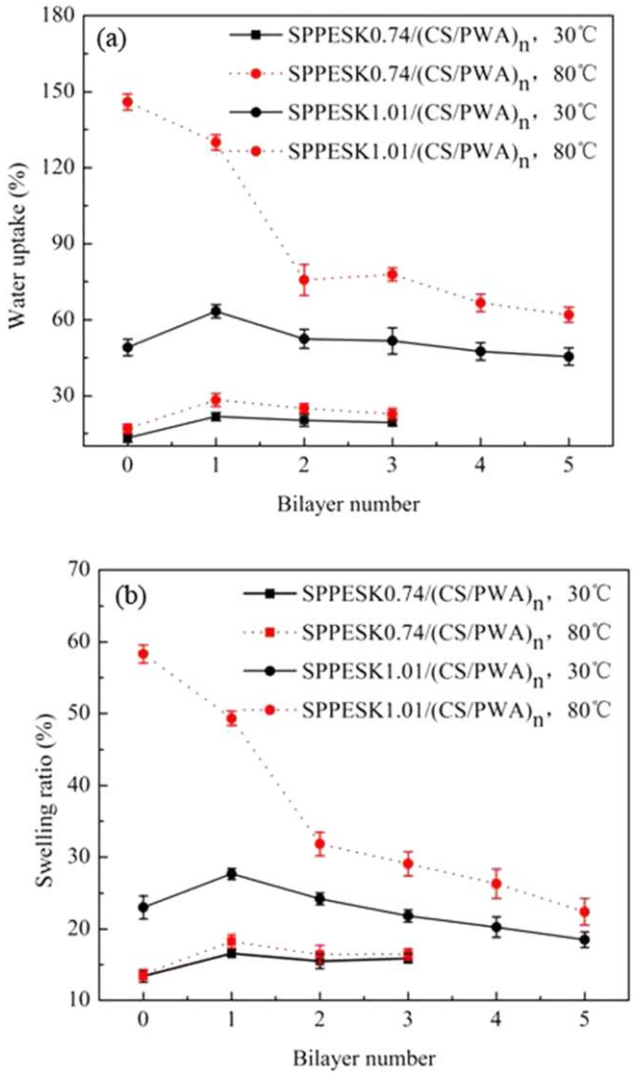

Figure 5. (a) Water uptake of the SPPESK and the SPPESK/(CS/PWA)$_n$ membranes; (b) Swelling ratio of the SPPESK and the SPPESK/(CS/PWA)$_n$ membranes. [Color figure can be viewed in the online issue, which is available at wileyonlinelibrary.com.]

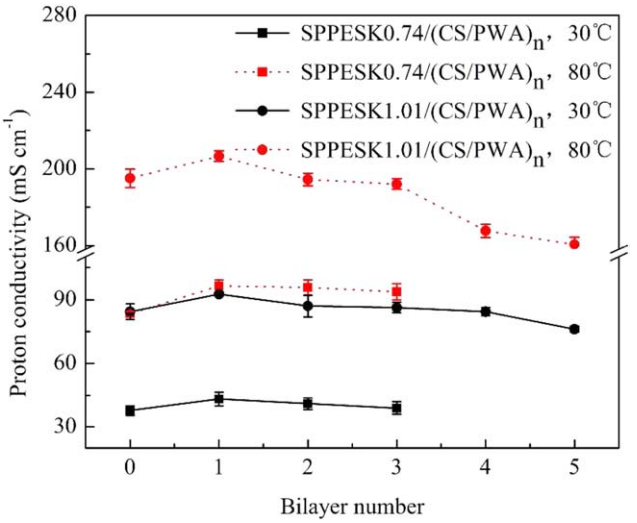

Figure 6. Proton conductivity of the SPPESK and the SPPESK/(CS/PWA)$_n$ membranes. [Color figure can be viewed in the online issue, which is available at wileyonlinelibrary.com.]

self-assembly is a promising technique in preparing and modifying PEMs for fuel cell applications.

Thermal Stability

TGA and DTG curves of the SPPESK and the SPPESK/(CS/PWA)$_n$ membranes are shown in Figure 9(a,b), respectively, and the corresponding data of 5% weight loss temperature ($T_{d5\%}$) and maximum weight loss rate temperature ($T_{d\text{-}max}$) are listed in Table I. According to Table I, $T_{d5\%}$ of the SPPESK0.74 membrane and the SPPESK0.74/(CS/PWA)$_3$ membrane are equal and that of SPPESK1.01/(CS/PWA)$_5$ membrane is 26°C higher compared with the SPPESK1.01 membrane. It demonstrates that the electrostatic interaction existing within the multilayer and between the multilayer film and substrate have a positive effect on the thermal stability of membrane with high DS. It is also

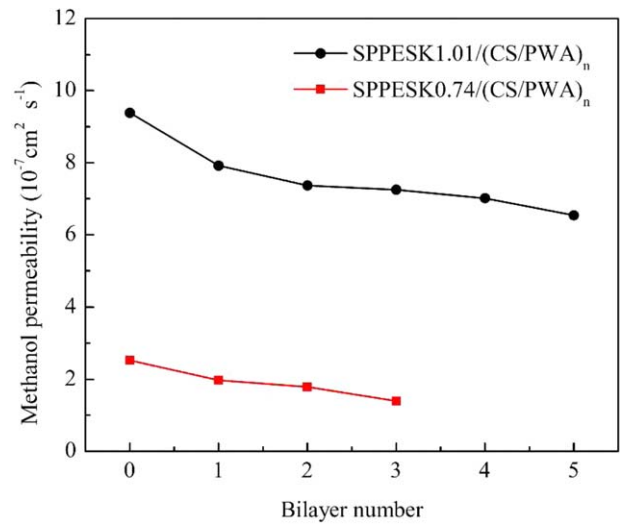

Figure 7. Methanol permeability of the SPPESK and the SPPESK/(CS/PWA)$_n$ membranes at 25°C. [Color figure can be viewed in the online issue, which is available at wileyonlinelibrary.com.]

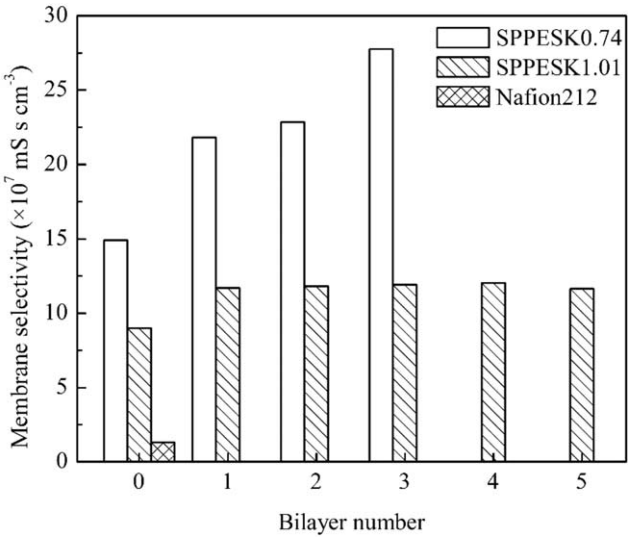

Figure 8. Selectivity of the SPPESK, the SPPESK/(CS/PWA)$_n$ membranes and Nafion212 at 25°C.

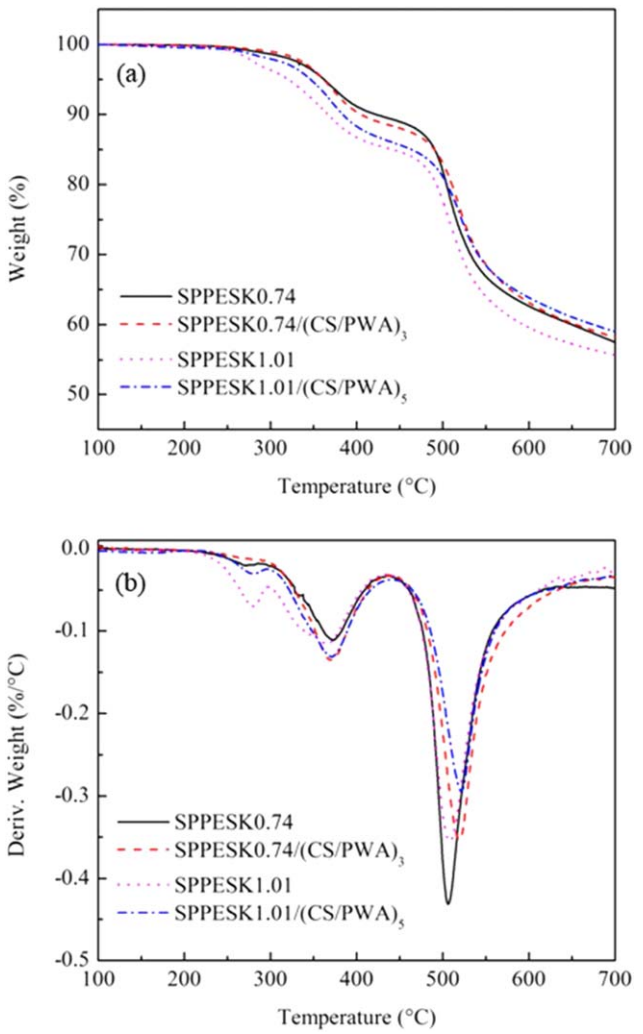

Figure 9. (a) TGA curves of the SPPESK and the SPPESK/(CS/PWA)$_n$ membranes; (b) DTG curves of the SPPESK and the SPPESK/(CS/PWA)$_n$ membranes. [Color figure can be viewed in the online issue, which is available at wileyonlinelibrary.com.]

Table I. Thermal Characteristic Temperature of the SPPESK and the SPPESK/$(CS/PWA)_n$ Membranes

Sample	$T_{d5\%}$ (°C)	$T_{d1\text{-}max}$ (°C)	$T_{d2\text{-}max}$ (°C)	$T_{d3\text{-}max}$ (°C)
SPPESK0.74	362	277	373	506
SPPESK0.74/$(CS/PWA)_3$	362	274	369	520
SPPESK1.01	321	280	366	508
SPPESK1.01/$(CS/PWA)_5$	347	279	371	522

$T_{d5\%}$: the 5% weight loss temperature; $T_{d\text{-}max}$: the max weight loss rate temperature.

observed from Figure 9 that both composite and pristine membranes possess three weight loss platforms. The first step with $T_{d1\text{-}max}$ (274–280°C) is attributed to the sulfonic acid group (—SO_3H) splitting off. Clearly, the loss weight of the SPPESK0.74 membrane is lower than that of the SPPESK1.01 membrane owing to its fewer —SO_3H groups. In addition, the composite membranes lose less weight than the pristine membrane, which can be interpreted that some —SO_3H groups combined with CS are not degraded. The second step with $T_{d2\text{-}max}$ (366-373°C) may be caused by the multilayer film and residual solvents.[9] The last step assigned to the degradation of backbone is at 505–525°C, and as seen, $T_{d3\text{-}max}$ of the SPPESK0.74/$(CS/PWA)_3$ membrane and the SPPESK1.01/$(CS/PWA)_5$ membrane are 520 and 522°C, respectively, about 14°C higher than that of the corresponding pristine membranes, indicating that membranes modified by LbL self-assembly exhibit highly thermal stability.

CONCLUSIONS

SPPESK composite membranes with two different DSs are prepared through the electrostatic LbL self-assembly method using polycation CS and negatively charged PWA. The characterizations of FTIR, SEM, and IEC have verified the success of the multilayer assembly. The membrane properties results indicate that the LbL self-assembly has different effects on the SPPESK membrane substrates of different DSs. It elevates proton conductivity of the SPPESK membrane of lower DS and enhances swelling stability of the SPPESK membrane of higher DS. For instance, proton conductivity of the SPPESK0.74/$(CS/PWA)_1$ membrane increases by 16% to 96.49 mS cm^{-1} (80°C), and swelling ratio of the SPPESK1.01/$(CS/PWA)_3$ membrane decreases from 58% (80°C) to 29%. It can be concluded that the LbL self-assembly has broadened the available DS range for fuel cell applications and reveals that an optimal DS must be determined according to the desired performance. Moreover, because of the electrostatic interaction and the ion cross-linking networks, permeability of the SPPESK0.74/$(CS/PWA)_3$ membrane and the SPPESK1.01/$(CS/PWA)_5$ membrane is reduced by 45 and 30%, respectively. In summary, the LbL self-assembly is proved to be a promising method in preparation and modification of PEMs.

ACKNOWLEDGMENTS

The authors thank the support of National Science Fund for Distinguished Young Scholars of China (Grant no.21125628) and National Natural Science Foundation of China (Grant no.21176044).

REFERENCES

1. Steele, B. C. H.; Heinzel, A. *Nature* **2001**, *414*, 345.
2. Oliveira, P. N.; Catarino, M.; Oliveira Mueller, C. M.; Brandao, L.; Pacheco Tanaka, D. A.; Bertolino, J. R.; Mendes, A. M.; Pires, A. T. N. *J. Appl. Polym. Sci.* **2014**, *131*, 40148.
3. Peighambardoust, S. J.; Rowshanzamir, S.; Amjadi, M. *Int. J. Hydrogen Energy* **2010**, *35*, 9349.
4. Du, L.; Yan, X. M.; He, G. H.; Wu, X. M.; Hu, Z. W.; Wang, Y. D. *Int. J. Hydrogen Energy* **2012**, *37*, 11853.
5. Wang, R. J.; Yan, X. M.; Wu, X. M.; He, G. H.; Du, L.; Hu, Z. W.; Tan, M. *J Polym. Sci. Part B: Polym. Phys.* **2014**, *52*, 1107.
6. Arico, A. S.; Srinivasan, S.; Antonucci, V. *Fuel Cells* **2001**, *1*, 133.
7. Lu, J. L.; Fang, Q. H.; Li, S. L.; Jiang, S. P. *J Membr. Sci.* **2013**, *427*, 101.
8. Gu, S.; He, G. H.; Wu, X. M.; Hu, Z. W.; Wang, L. L.; Xiao, G. K.; Peng, L. *J. Appl. Polym. Sci.* **2010**, *116*, 852.
9. Wu, X. M.; He, G. H.; Gu, S.; Chen, W.; Yao, P. J. *J. Appl. Polym. Sci.* **2007**, *104*, 1002.
10. Wang, J. T.; Jiang, S.; Zhang, H.; Lv, W. J.; Yang, X. L.; Jiang, Z. Y. *J. Membr. Sci.* **2010**, *364*, 253.
11. Fu, T. Z.; Wang, J.; Ni, J.; Cui, Z. M.; Zhong, S. L.; Zhao, C. J.; Na, H.; Xing, W. *Solid State Ionics* **2008**, *179*, 2265.
12. Su, Y. H.; Liu, Y. L.; Sun, Y. M.; Lai, J. Y.; Guiver, M. D.; Gao, Y. *J. Power Sources* **2006**, *155*, 111.
13. Gu, S.; He, G. H.; Wu, X. M.; Guo, Y. J.; Liu, H. J.; Peng, L.; Xiao, G. K. *J. Membr. Sci.* **2008**, *312*, 48.
14. Wu, X. M.; He, G. H.; Gu, S.; Hu, Z. W.; Yao, P. J. *J. Membr. Sci.* **2007**, *295*, 80.
15. Hu, Z. W.; He, G. H.; Gu, S.; Liu, Y. F.; Wu, X. M. *J. Appl. Polym. Sci.* **2014**, *131*, 39852.
16. Nagarale, R. K.; Gohil, G. S.; Shahi, V. K. *J. Membr. Sci.* **2006**, *280*, 389.
17. Xiang, Y.; Lu, S.; Jiang, S. P. *Chem. Soc. Rev.* **2012**, *41*, 7291.
18. Zhao, Q.; An, Q. F.; Ji, Y.; Qian, J.; Gao, C. *J Membr. Sci.* **2011**, *379*, 19.
19. Iost, R. M.; Crespilho, F. N. *Biosens. Bioelectron.* **2012**, *31*, 1.
20. Hammond, P. T. *Curr. Opin. Colloid Interface Sci.* **1999**, *4*, 430.
21. Perumal, B.; Sangeetha, D. *Int. J. Polym. Mater.* **2013**, *62*, 462.
22. Xiang, Y.; Zhang, J.; Liu, Y.; Guo, Z. B.; Lu, S. F. *J. Membr. Sci.* **2011**, *367*, 325.
23. Wang, J.; Zhao, C. J.; Lin, H. D.; Zhang, G.; Zhang, Y.; Ni, J.; Ma, W. J.; Na, H. *J. Power Sources* **2011**, *196*, 5432.

24. Zhao, C. J.; Lin, H. D.; Zhang, Q.; Na, H. *Int. J. Hydrogen Energy* **2010**, *35*, 10482.
25. Zhao, C. J.; Lin, H. D.; Cui, Z. M.; Li, X. F.; Na, H.; Xing, W. *J. Power Sources* **2009**, *194*, 168.
26. Ariga, K.; Hill, J. P.; Ji, Q. *Phys. Chem. Chem. Phys.* **2007**, *9*, 2319.
27. Quinn, J. F.; Johnston, A. P.; Such, G. K.; Zelikin, A. N.; Caruso, F. *Chem. Soc. Rev.* **2007**, *36*, 707.
28. Jiang, S. P.; Tang, H. L. *Colloids Surf. A* **2012**, *407*, 49.
29. Argun, A. A.; Ashcraft, J. N.; Hammond, P. T. *Adv. Mater.* **2008**, *20*, 1539.
30. Deligöz, H.; Yılmaztürk, S.; Karaca, T.; Özdemir, H.; Koç, S. N.; Öksüzömer, F.; Durmuş, A.; Gürkaynak, M. A. *J. Membr. Sci.* **2009**, *326*, 643.
31. Yılmaztürk, S.; Deligöz, H.; Yılmazoğlu, M.; Damyan, H.; Öksüzömer, F.; Koç, S. N.; Durmuş, A.; Gürkaynak, M. A. *J. Membr. Sci.* **2009**, *343*, 137.
32. Yang, M.; Lu, S.; Lu, J.; Jiang, S. P.; Xiang, Y. *Chem. Commun (Camb).* **2010**, *46*, 1434.
33. Chen, L.; Tang, H. L.; Li, J. R.; Pan, M. *Int. J. Energy Res.* **2013**, *37*, 879.
34. Cui, Z.; Xing, W.; Liu, C.; Liao, J.; Zhang, H. *J. Power Sources* **2009**, *188*, 24.
35. Jiang, Z.; Zheng, X.; Wu, H.; Wang, J.; Wang, Y. *J. Power Sources* **2008**, *180*, 143.
36. Hammond, P. T. *AIChE. J.* **2011**, *57*, 2928.
37. Masatomi, I.; Tetsuya, S.; Masaaki, I.; Ryuichi, S.; Hiroshi, N.; Tomio, T. *J. Antibiot.* **1999**, *52*, 775.
38. Tsai, J. C.; Lin, C. K. *J. Taiwan Inst. Chem.* **2011**, *42*, 281.
39. Xu, D.; Zhang, G.; Zhang, N.; Li, H.; Zhang, Y.; Shao, K.; Han, M.; Lew, C. M.; Na, H. *J. Mater. Chem.* **2010**, *20*, 9239.
40. Wan, C. H.; Lin, M. T. *J. Power Sources* **2013**, *222*, 470.
41. Zhang, H.; Huang, H.; Shen, P. K. *Int. J. Hydrogen Energy* **2012**, *37*, 6875.
42. Gu, S.; He, G. H.; Wu, X. M.; Li, C. N.; Liu, H. J.; Lin, C.; Li, X. C. *J. Membr. Sci.* **2006**, *281*, 121.